Intercellular mRNA trafficking via membrane nanotube-like extensions in mammalian cells

Gal Haimovich[a,b], Christopher M. Ecker[c], Margaret C. Dunagin[c], Elliott Eggan[c], Arjun Raj[c], Jeffrey E. Gerst[a,1], and Robert H. Singer[b,d,1]

[a]Department of Molecular Genetics, Weizmann Institute of Science, Rehovot 7610001, Israel; [b]Department of Anatomy and Structural Biology, Albert Einstein College of Medicine, Bronx, NY 10461; [c]Department of Bioengineering, University of Pennsylvania, Philadelphia, PA 19104; and [d]Janelia Research Campus of the Howard Hughes Medical Institute, Ashburn, VA 20147

Contributed by Robert H. Singer, September 26, 2017 (sent for review April 18, 2017; reviewed by Jennifer Lippincott-Schwartz, Peter Walter, and Jonathan S. Weissman)

RNAs have been shown to undergo transfer between mammalian cells, although the mechanism behind this phenomenon and its overall importance to cell physiology is not well understood. Numerous publications have suggested that RNAs (microRNAs and incomplete mRNAs) undergo transfer via extracellular vesicles (e.g., exosomes). However, in contrast to a diffusion-based transfer mechanism, we find that full-length mRNAs undergo direct cell–cell transfer via cytoplasmic extensions characteristic of membrane nanotubes (mNTs), which connect donor and acceptor cells. By employing a simple coculture experimental model and using single-molecule imaging, we provide quantitative data showing that mRNAs are transferred between cells in contact. Examples of mRNAs that undergo transfer include those encoding GFP, mouse β-actin, and human Cyclin D1, BRCA1, MT2A, and HER2. We show that intercellular mRNA transfer occurs in all coculture models tested (e.g., between primary cells, immortalized cells, and in cocultures of immortalized human and murine cells). Rapid mRNA transfer is dependent upon actin but is independent of de novo protein synthesis and is modulated by stress conditions and gene-expression levels. Hence, this work supports the hypothesis that full-length mRNAs undergo transfer between cells through a refined structural connection. Importantly, unlike the transfer of miRNA or RNA fragments, this process of communication transfers genetic information that could potentially alter the acceptor cell proteome. This phenomenon may prove important for the proper development and functioning of tissues as well as for host–parasite or symbiotic interactions.

membrane nanotubes | MS2 | smFISH | β-actin mRNA

An essential aspect of multicellular organisms is the ability of cells to communicate with each other over both long and short distances to coordinate cellular and organ processes. Although most studies have focused on small molecule- or protein-based intercellular communication, little is known about whether RNA molecules act by themselves as mediators of communication. Earlier reports suggested that RNAs may undergo transfer from one cell to another (1–3). However, only recently has it become evident that the extracellular fluids of animals (e.g., saliva, plasma, milk, and urine) contain RNAs, including mRNAs (or fragments thereof) and miRNAs. These RNAs are mainly found in extracellular nanovesicles (EVs) such as exosomes (4), although free extracellular ribonucleoprotein (RNP) particles have been identified (5). By using DNA microarrays (4, 6, 7) or RNA-sequencing (RNA-seq) (8), the content of EVs was shown to include a multitude of mRNAs and miRNAs. Thus, it has been proposed that the transfer of RNA between donor and acceptor cells could play an important physiological role.

However, examples of exosome-mediated intercellular mRNA transfer and its effects are few (4, 9–12). Only two studies provide qualitative evidence for the possible translation of transferred mRNA in recipient cells (4, 12), and no follow-up research was performed. In particular, there is a lack of quantitative data regarding the number and fate of transferred mRNA molecules at the single-cell level. Moreover, the existence of multiple types of EVs (e.g., exosomes, microvesicles, and apoptotic bodies) that can contain different kinds of cargo, including DNA (13), complicates the study and understanding of this process. In addition, it has been demonstrated that exosomes are transported into lysosomes upon internalization by recipient cells (13–15), and it is unclear how their RNA content reaches sites of translation within the cytoplasm.

Another consideration is that while the abundance of mRNAs in terms of species per copy number in EVs is unknown, the small volume of exosomes might not allow more than a limited number of mRNA molecules per exosome. The presence of full-length, functional mRNAs in exosomes was demonstrated in a few studies (4, 12), whereas others suggest that exosomes contain mainly RNA fragments (16–18). Indeed, one study found that only short mRNA fragments (<500 nt) are efficiently loaded into EVs, compared with longer transcripts (>1,500 nt) (17). Recent reports also suggest that miRNAs are present in very low abundance in EVs (i.e., individual miRNAs may range between 10^{-4} and 60 miRNA molecules per exosome in a given extracellular fluid) (19, 20), suggesting that miRNA transfer via EVs might have little influence on recipient cells unless selective mechanisms for uptake exist. Overall, these results suggest that a large number of EVs containing specific mRNAs (or mRNA fragments) or miRNAs might be necessary to significantly affect

Significance

mRNA molecules convey genetic information within cells, beginning from genes in the nucleus to ribosomes in the cell body, where they are translated into proteins. Here we show a mode of transferring genetic information from one cell to another. Contrary to previous publications suggesting that mRNAs transfer via extracellular vesicles, we provide visual and quantitative data showing that mRNAs transfer via membrane nanotubes and direct cell-to-cell contact. We predict that this process has a major role in regulating local cellular environments with respect to tissue development and maintenance and cellular responses to stress, interactions with parasites, tissue transplants, and the tumor microenvironment.

Author contributions: G.H., A.R., and R.H.S. designed research; G.H., C.M.E., M.C.D., and E.E. performed research; G.H. contributed new reagents/analytic tools; G.H., C.M.E., M.C.D., and E.E. analyzed data; and G.H., A.R., J.E.G., and R.H.S. wrote the paper.

Reviewers: J.L.-S., Howard Hughes Medical Institute Janelia Research Campus; P.W., University of California, San Francisco; and J.S.W., University of California, San Francisco.

The authors declare no conflict of interest.

[1]To whom correspondence may be addressed. Email: jeffrey.gerst@weizmann.ac.il or robert.singer@einstein.yu.edu.

This article contains supporting information online at www.pnas.org/lookup/suppl/doi:10.1073/pnas.1706365114/-/DCSupplemental.

the physiology of recipient cells. Additionally, other modes of mRNA transfer were not investigated. Thus, an unbiased quantitative approach is needed to determine if mRNA is indeed transferrable and, if so, how it is transferred, and how much is transferred.

To study intercellular mRNA transfer in a quantitative and unbiased manner, we employed a simple strategy that is depicted in Fig. 1 *A* and *B*. In this model, "donor" and "acceptor" cells are cocultured together, and the transfer of specific mRNA species from donors to acceptors is visualized and quantified by single-molecule FISH (smFISH) (21, 22) or live imaging using the MS2 aptamer system (23). Donor and acceptor pairings can consist of cell types from any typical mammalian species (e.g., rat, mouse, human), provided that the query mRNA is expressed only in the donor cells. By using this model, we discovered that mRNAs can transfer between cells, and we provide absolute quantitative data on the number of transferred mRNA molecules per cell under different culture conditions.

We show that mRNA transfer requires direct cell-to-cell contact and that it appears to occur via membrane nanotubes (mNTs; also known as "tunneling nanotubes") and not by diffusion. mNTs are long and thin cytoplasmic projections involved in direct contact-dependent intercellular communication between eukaryotic cells. mNTs were shown to be open-ended (24) and seem to allow the direct flow of cytoplasmic content between connected cells (25, 26). Indeed, mNTs support cell-to-cell transfer of small molecules, proteins, prions, viral particles, vesicles, and organelles in a variety of cell types (24–35). Here we demonstrate that mNTs appear to be involved in the transfer of mRNA molecules and identify mRNAs encoding a wide variety of proteins that undergo intercellular transfer in in vitro culture conditions.

Results

mRNA Can Transfer Between Cells. To determine whether cell–cell mRNA transfer occurs, immortalized WT mouse embryonic fibroblasts (MEFs) were cocultured with immortalized MEFs derived from a homozygous transgenic mouse that harbors 24 repeats of the MS2-coat protein (MCP)–binding sequence (MBS) at the 3′ UTR of the endogenous alleles of β-actin (referred to here as "MBS MEFs") (23). smFISH with MBS-specific probes was used to analyze the number of β-actin–MBS mRNAs detected, and quantitation was performed using in-laboratory programs or FISH-quant (FQ) (*SI Materials and Methods* and Fig. S1 *A* and *B*) (36). MBS MEFs showed up to several thousand distinct FISH spots in each cell as well as bright nuclear foci representing transcription sites (Fig. 1*C*, *Left*, Fig. S1*C*, and Dataset S1) (23). Immortalized MBS MEFs are tetraploid and have up to four transcription sites (23). As expected, β-actin–MBS mRNAs and transcription sites were not detected in WT MEFs cultured alone (Fig. 1*C*, *Center*). However, when cocultured with MBS MEFs for 24 h, WT cells acquired MBS-labeled mRNAs (Fig. 1*C*, *Right*) at an average (± SEM) of 45 ± 4 mRNAs per cell and as many as ∼190 mRNAs per cell (Fig. 1*D* and Dataset S1).

To determine the global rate of mRNA transfer, we measured the number of transferred β-actin–MBS mRNAs in WT MEFs at 0.5, 1.5, 2.5, and 4.5 h after adding MBS MEFs to the culture. Under these conditions, MBS MEFs attached to the fibronectin (FN)-coated glass surface within 15–20 min. We detected transferred mRNA within 30 min of coculture (i.e., 10–15 min after MBS MEFs attached to the surface). The number of transferred mRNAs increased with time until reaching a plateau at 2.5 h after coculture (Fig. 1*E* and Dataset S1).

Zipcode-binding protein 1 (ZBP1) is an RNA-binding protein (RBP) previously shown to be required for β-actin mRNA localization to the leading edge and focal adhesions in fibroblasts (37, 38) and to dendrites in neurons (39, 40). However, the absence of ZBP1 in the donor MBS MEFs (i.e., immortalized β-actin–MBS ZBP1$^{-/-}$ MEFs) did not hinder mRNA transfer to immortalized acceptor WT MEFs (Fig. S1*D* and Dataset S1).

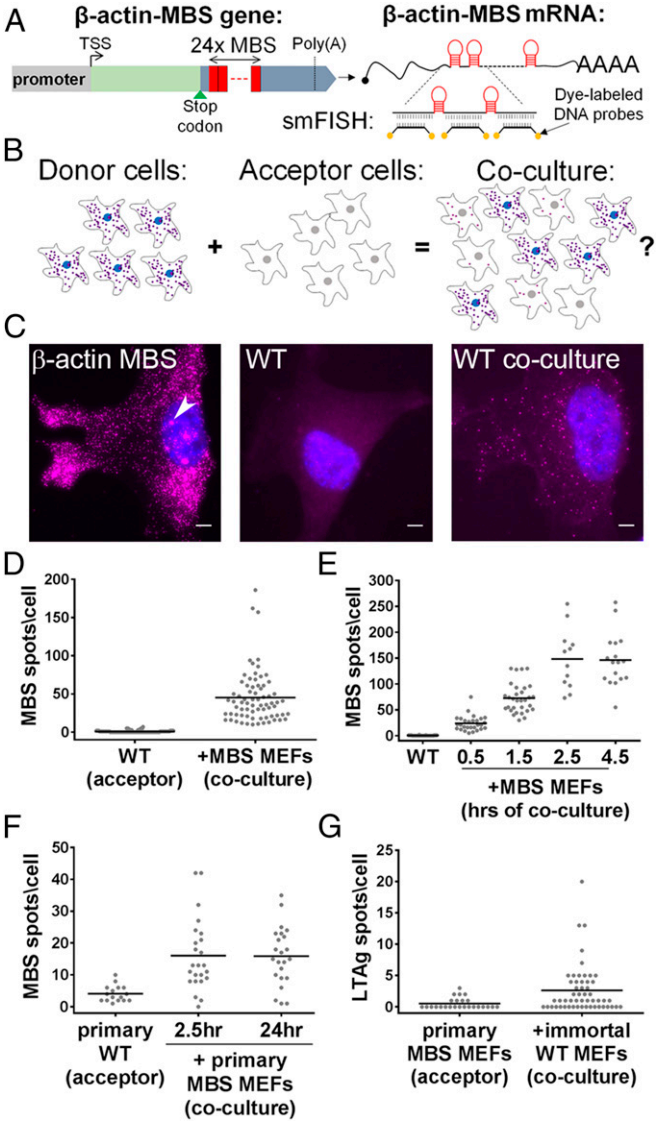

Fig. 1. Detection of β-actin–MBS mRNA transfer by smFISH. (*A*) A schematic depicting the β-actin–MBS gene (*Left*) and resulting mRNA (*Right*). mRNA detection was accomplished using smFISH with fluorescence-labeled DNA probes against the MBS sequence (aka "MBS probes"). Poly(A), polyadenylation site; TSS, transcription start site. (*B*) A schematic illustrating the basic experimental set-up. Donor cells (*Left*) that express a unique mRNA (e.g., β-actin–MBS; shown as small purple dots) were cocultured with naive acceptor cells (*Middle*) that lack this mRNA. If mRNAs undergo transfer from donor to acceptor cells, coculture yields labeling of the acceptor cells (*Right*). Each cell type was also cultured separately to assess mRNA-expression levels in donor cells or background staining in acceptor cells. (*C*) smFISH images of an immortalized donor MBS MEF, immortalized acceptor WT MEF, and acceptor WT MEF in coculture. Labels: blue, DAPI staining of the nucleus; magenta, Cy3-tagged MBS probes. The arrowhead indicates a transcription site. (Scale bars: 5 μm.) (*D*) Distribution of the number of β-actin–MBS mRNA spots observed in immortalized WT MEFs (expressing low levels of GFP) cultured alone or cocultured with donor MBS MEFs for 24 h. Each dot in *D*–*G* represents the score of the number of mRNAs detected in a single cell as obtained by smFISH. The horizontal bars in *D*–*G* indicate mean number of spots per acceptor cell. (*E*) Distribution of the number of β-actin–MBS mRNA spots in WT MEFs as a function of time after coculture with donor MBS MEFs. (*F*) Distribution of the number of β-actin–MBS mRNA spots in primary WT MEFs cultured alone or cocultured for 2.5 or 24 h with primary donor MBS MEFs. (*G*) Distribution of the number of LTag mRNA spots in primary MBS MEFs cocultured with LTag-immortalized donor WT MEFs for 24 h. See Dataset S1 for data on the number of cells scored, mean, SEM, and *P* values for each experiment.

To determine that mRNA transfer is not due to immortalization, we examined whether it occurs between primary cells. Primary MEFs derived from WT or MBS mice were cocultured for either 2.5 or 24 h, and smFISH was performed to detect β-actin–MBS mRNA transfer. Similar to immortalized MEFs, transferred β-actin–MBS mRNA was detected in cocultured primary WT MEFs (Fig. 1*F* and Dataset S1). This indicated that intercellular RNA transfer is not unique to immortalized cells. Cocultures of primary MEFs and immortalized MEFs yielded a twofold higher level of mRNA transfer compared with primary coculture (Fig. S1*E* and Dataset S1). Coculturing primary and immortalized MEFs also allowed us to test the transfer of a second mRNA, SV40 large T antigen (LTag) mRNA, which is expressed only in the immortalized cells (Fig. S2; see Dataset S1 for expression levels in donor cells). By employing LTag-specific smFISH probes, we could detect the transfer of LTag mRNA from immortalized to primary MEFs (Fig. 1*G* and Dataset S1). This indicates that transfer is not unique to β-actin mRNA or to MBS-labeled mRNAs.

FISH experiments using Cy3-labeled MBS- and Cy5-labeled ORF-specific probes showed that an average of 3.5 ± 0.4% of the total β-actin mRNA found in WT MEFs (as detected by ORF-specific probes) was transferred from donor MBS cells (Fig. S3 *A* and *B* and Dataset S1). In these FISH experiments, most of the MBS spots detected in MBS MEFs were colocalized with ORF spots, although there were a few single-color–labeled spots (Fig. S3*C*). It is important to note that many MBS spots detected in WT MEFs also colocalized with ORF spots (Fig. S3 *D* and *E*), indicating that the transferred β-actin–MBS mRNAs detected in acceptor cells constituted full-length transcripts and not solely 3′ UTR or MBS fragments.

mRNA Transfer Occurs in Heterologous Human/Murine Cell Cocultures. To test the generality of this process, we first determined if β-actin–MBS mRNA from MEFs can transfer to other cell types, including human cells. We therefore cocultured MBS MEFs with a human embryonic kidney cell line (HEK293T) and examined these cells for β-actin–MBS mRNA. Indeed, we found that β-actin–MBS mRNA can transfer from murine to human cells (Fig. 2*A* and Dataset S1). Although the mean amount of endogenous β-actin mRNA levels in MEFs is about threefold higher than in HEK293T cells (Fig. S3*F* and Dataset S1), the transferred mRNA constitutes 4.5 ± 0.6% of the β-actin ORF spots in HEK293T cells (Fig. S3 *G* and *H* and Dataset S1). This is similar in percentage to the amount of transferred mRNA between MEFs, which suggests that this is either a regulated or a limited process. β-Actin–MBS mRNA transfer was also detected in cocultures of MBS MEFs with the human osteosarcoma (U2OS) or adenocarcinoma (SKBR3) cell lines (Fig. S4 *A* and *B* and Dataset S1). This shows that the mechanism of transfer is conserved and confers the murine–human exchange of mRNA. Reciprocal transfer experiments using human-specific probes showed that an endogenous mRNA, such as BRCA1 mRNA (Fig. S2 and Dataset S1), transferred from HEK293T or HEK293 cells to MEFs (Fig. 2*B* and Dataset S1). Likewise, endogenously expressed SERP2, MITF, and MT2A mRNAs (Fig. S2 and Dataset S1) transferred from human melanoma cells (WM983b–GFP) to murine embryonic fibroblasts (NIH 3T3) in coculture (Fig. 2 *C*–*E* and Dataset S1). The transfer of the ectopically expressed GFP mRNA (Fig. S2 and Dataset S1) could also be detected both in human–murine and human–human cocultures (Fig. S4 *C* and *D* and Dataset S1). For these experiments, we employed smFISH probes that tiled the entire length of the transcript for the non–MBS-labeled mRNAs. In some cases [e.g., GFP (Fig. S4*E*) and SERP2, MITF, and MT2A (Fig. S2*B*)], dual-color probe sets (41) were used to ascertain the specific identification of these mRNAs, since two-color colocalization enhances the probability that the signal is specific. These approaches strongly indicate that full-length mRNAs underwent transfer. To test for transfer of a different type of RNA molecule, we also examined by dual-color smFISH whether a highly expressed (e.g., >2,000 copies per cell) human-specific long noncoding RNA (lncRNA), MALAT1 (41), underwent transfer, but we observed the transfer of only one or two molecules in a small percentage (~8%) of acceptor cells (Fig. S4*F* and Dataset S1). At this moment we cannot determine whether the lack of appreciable MALAT1 RNA transfer is due to its localization in the nucleus (41) or its specific function and/or regulation.

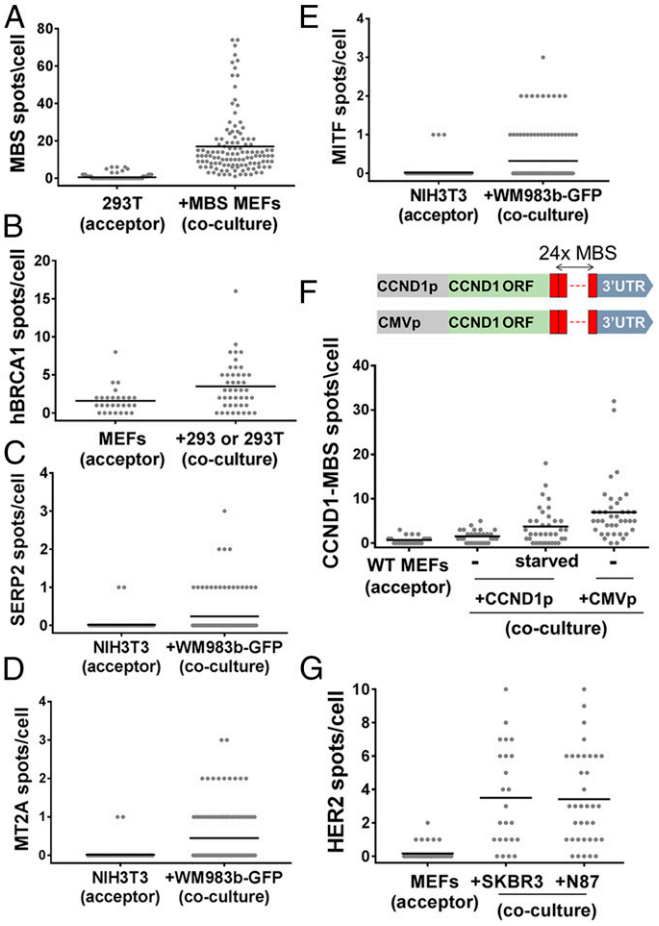

Fig. 2. Transfer of mRNAs in human–murine cocultures. (*A*) Distribution of the number of β-actin–MBS mRNA spots in HEK293T cells that were cocultured with donor MBS MEFs for 24 h. In all panels, each dot represents the score of a single cell using smFISH, and the horizontal bars indicate the mean number of spots per acceptor cell. (*B*) Distribution of the number of endogenously expressed human BRCA1 mRNA spots in WT MEFs cocultured for 24 h with donor HEK293T or HEK293 cells, as detected using sequence-specific probes against BRCA1. (*C*–*E*) Distribution of the number of SERP2 (*C*), MITF (*D*), and MT2A (*E*) mRNA spots in NIH 3T3 cells that were cocultured with donor WM983b–GFP human melanoma cells for 48 h, as detected using sequence-specific probes. Only dual-color spots were considered legitimate mRNA spots. (*F*) Distribution of the number of CCND1–MBS mRNA spots in WT MEFs cocultured for 7 h with donor HEK293 cells expressing CCND1–MBS mRNA from CCND1p or CMVp. Starved WT MEFs were serum-starved overnight before coculture. MBS probes were used for the detection of CCND1–MBS mRNA. The diagram above the plot illustrates the CCND1–MBS gene under the two different promoters in the HEK293 cell lines. (*G*) Distribution of the number of endogenously expressed human HER2 mRNA spots in MEFs cocultured for 3 h with donor SKBR3 or NCI-N87 cells, using sequence-specific probes. See Dataset S1 for data on the number of cells scored, mean, SEM, and *P* values.

Gene Expression in Donor Cells May Influence mRNA Transfer. In contrast to β-actin–MBS mRNA, which undergoes transfer at tens to hundreds of molecules per cell (Figs. 1 *C*–*F* and 2*A* and

Figs. S1 *D* and *E*, S3 *B* and *H*, and S4 *A* and *B*), only a small amount of the other RNAs tested were transferred (Figs. 1*G* and 2 *B*–*E* and Fig. S4 *C* and *D*). Furthermore, primary MBS MEFs, which express less β-actin–MBS mRNA than immortalized MBS MEFs (Fig. S1), also exhibited less transfer (Fig. 1*F* and Fig. S1*E*). Thus, we hypothesized that mRNA-expression levels in donor cells might affect the absolute number of transferred RNAs.

To test whether gene expression affects mRNA transfer, two HEK293 cell lines that express MBS-labeled cyclin D1 (CCND1–MBS) mRNA from either its endogenous promoter (CCND1p) or a CMV promoter (CMVp) were obtained (42). As expected, CMVp induced higher levels of expression of CCND1–MBS mRNA in donor cells compared with CCND1p (Fig. S2 and Dataset S1). We cocultured WT MEFs with either of these cell lines and compared the level of CCND1–MBS mRNA transfer. In agreement with our hypothesis, more RNA transfer was detected when the MEFs were cocultured with HEK293 cells bearing CMVp–CCND1–MBS (Fig. 2*F* and Dataset S1).

To explore this issue further, we examined the transfer of HER2 mRNA from human cell lines to MEFs. We used two epithelial cell lines having different expression levels of HER2: gastric carcinoma cells (NCI-N87; 316 ± 22 mRNAs per cell) and SKBR3 cells (611 ± 36 mRNAs per cell) (Fig. S2 and Dataset S1). We observed mRNA transfer in both cases, and, despite the elevated expression of HER2 mRNA in SKBR3 cells, we observed the same low level of transfer (e.g., ∼3.5 mRNAs per cell) (Fig. 2*G* and Dataset S1). Given that HER2 mRNA is highly expressed in the donor cells, similar to β-actin, this result indicates that factors other than gene-expression level may influence transfer.

Stress Conditions Affect mRNA Transfer. To determine whether intercellular mRNA transfer is affected by external physiological conditions, we examined the effect of stress on mRNA transfer. In these experiments, either donor or acceptor cells were exposed to stress (e.g., heat shock, oxidative stress, protein-folding stress, or serum starvation) before coculture. Cells were relieved from the stress, and the reciprocal cells (i.e., unstressed acceptor or donor cells) were plated on top. Under these conditions, recovery from heat shock inhibited mRNA transfer, whereas recovery from oxidative stress (H_2O_2 treatment), protein-folding stress (DTT treatment), or serum starvation increased the extent of mRNA transfer (Figs. 2*G* and 3 and Dataset S1). Interestingly, stress conditions modulated mRNA transfer mostly when applied to the acceptor cells. Thus, different stresses may make cells either less or more receptive to mRNA transfer but have little effect on the capacity of donor cells to transfer mRNA once the stress is relieved. This occurred even though β-actin–MBS mRNA levels increased in the stressed donor cells after they were allowed to recover (Fig. S1). This also implies that mRNA-expression levels alone may not be the only parameter that influences transfer. We next tested whether translational stress inhibits mRNA transfer. We found that β-actin–MBS mRNA transfer was not inhibited by cycloheximide (Fig. S5*A* and Dataset S1), a translation inhibitor, indicating that this process does not require de novo protein synthesis.

mRNA Transfer Requires Direct Cell-to-Cell Contact. The isolation and characterization of exosomes and other EVs from different cell types has revealed that these vesicles may contain miRNAs and mRNA (or at least mRNA fragments) and therefore could serve as a means of mRNA transfer between cells (4, 12). Thus, we speculated that intercellular mRNA transfer is mediated by EVs that convey their contents by diffusion through the medium and uptake into acceptor cells. To test this hypothesis, we transferred "conditioned" medium from donor-cell cultures (e.g., MBS MEFs or WM983b–GFP cells) to acceptor-cell cultures (e.g., WT MEFs or WM983b cells, respectively) and looked for transferred β-actin–MBS or GFP mRNA in the acceptor cells

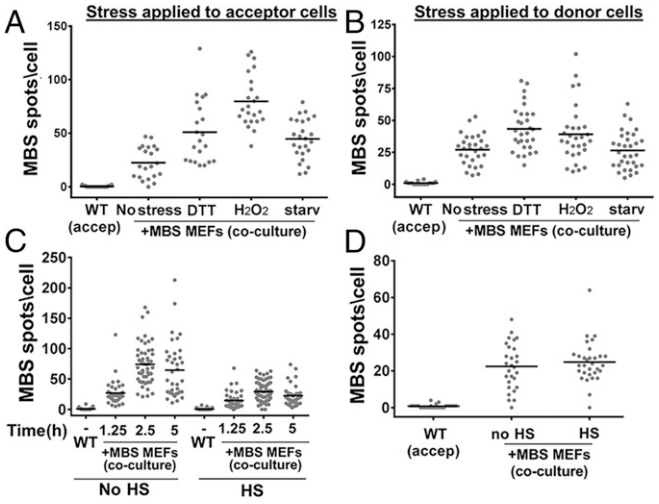

Fig. 3. Stress affects β-actin–MBS mRNA transfer. (*A* and *B*) Acceptor WT MEFs (*A*) or donor β-actin–MBS MEFs (*B*) were either left untreated (No stress) or were treated for 1.5 h with 1 mM DTT, 1 mM H_2O_2, or serum starvation (Starv) before scoring for mRNA transfer by smFISH with MBS probes. (*C* and *D*) Acceptor WT MEFs (*C*) or donor β-actin–MBS MEFs (*D*) were exposed to heat shock (HS, 42 °C) for 1 h or were left untreated (No HS). Following stress, the reciprocal cell line was plated, and coculture was maintained under stress-free conditions for 2.5 h (*A*, *B*, and *D*) or for the indicated times (*C*). β-Actin–MBS mRNA transfer was detected by smFISH using MBS probes, as described in Fig. 1. For the heat-shock experiments, we verified the heat-shock response by detecting heat shock-induced expression of HSP70 mRNA by smFISH. In all panels, the horizontal bar indicates the mean number of MBS spots per acceptor cell. See also Dataset S1 for data on the number of cells scored, mean, SEM, and *P* values.

following 1.5–2.5 or 24 h of incubation. Transferred mRNA molecules were not detected in the acceptor cells (Fig. 4 *A* and *B* and Dataset S1), indicating that the mode of transfer is not via the growth medium. Consequently, to determine if mRNA transfer is mediated by physical contact, donor and acceptor cells were cocultured under conditions that prevent contact between cells but allow the sharing of diffusible materials. We used two different approaches. The first approach, which we term "tripod," is illustrated in Fig. 4*C*. In this system, in which donor- and acceptor-cell layers are physically separated by several millimeters, any type of particle can diffuse across the medium. The second approach, termed "transwell", utilized a physical barrier to separate the cell layers and exclude the transfer of particles >0.4–5 μm (Fig. 4*D*). In either case, little to no evidence for mRNA transfer was detected, and transfer was observed only under coculture conditions that allowed physical contact (Fig. 4 *A* and *B* and Dataset S1). Last, exosomes were directly isolated from WM983b–GFP cells. These exosomes were 40–60 nm in diameter (Fig. S5*B*) and contained primarily small RNAs (<200 nt) (Fig. S5*C*). The isolated exosomes were applied to GFP-negative WM983b cells. After 24 h of incubation with the acceptor cells, no appreciable mRNA transfer was detected (Fig. 4*B* and Dataset S1). Thus, mRNA transfer appears to require cell–cell contact.

Although the release of mRNAs from dying cells might also allow transfer, we observed little cell death in our MEF coculture experiments (∼3%). Nevertheless, we tested whether cell death contributes to transfer by pretreating donor MBS MEFs with H_2O_2 (3%, 1.5 h) to induce oxidative stress and apoptosis. This treatment resulted in ∼45% cell death during the subsequent 2.5 h of incubation in cocultures with acceptor MEFs using the tripod approach described above. We observed only a slight increase in transferred β-actin–MBS mRNA levels in acceptor MEFs (Fig. 4*A* and Dataset S1). This level of transfer is far less

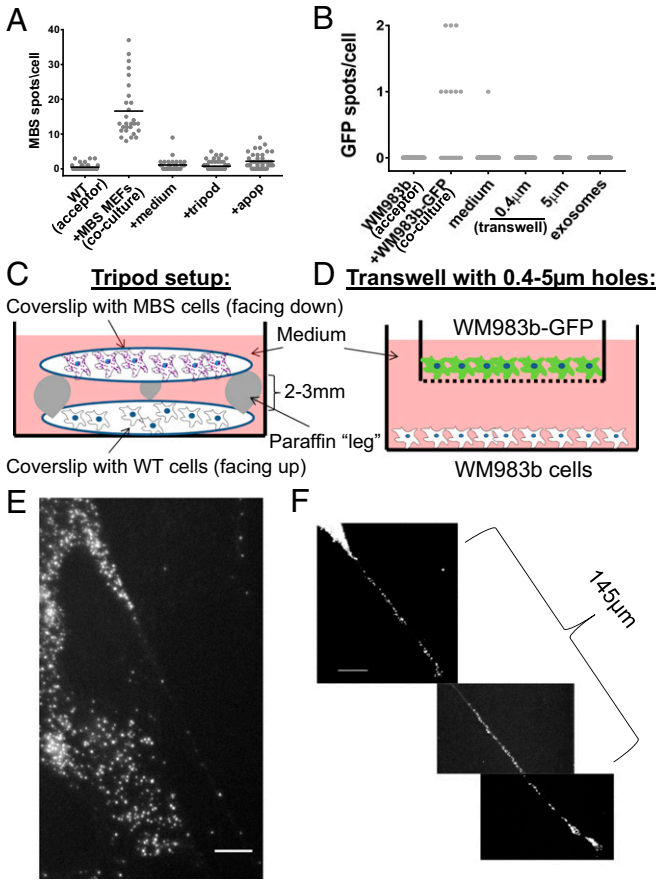

Fig. 4. Intercellular mRNA transfer requires direct cell-to-cell contact. (*A*) Distribution of the number of β-actin–MBS mRNA spots in acceptor WT MEFs cocultured with donor β-actin–MBS cells (coculture, as shown in Fig. 1), incubated with medium collected from an overnight culture of MBS MEFs (+medium), as shown in the tripod set-up (+tripod), or as shown in the tripod set-up with dying cells (+apop). Apoptosis was induced in donor MBS cells by pretreatment with 3% H_2O_2 before coculture in the tripod set-up with WT MEFs. Incubation time was 2 h for each treatment. Horizontal bars indicate the mean number of MBS spots per acceptor cell. (*B*) Distribution of the number of GFP mRNA spots in acceptor WM983b cells cocultured with donor WM983b–GFP cells (coculture). WM983b cells were incubated with medium collected from an overnight culture of WM983b–GFP cells (medium) in the transwell set-up using either 0.4-μm or 5-μm pores or with exosomes isolated from WM983b–GFP cells. Incubation time was 24 h for each treatment. Detection was performed using GFP-specific probes. (*C*) A schematic depicting the tripod set-up. Donor and acceptor cells grown separately on glass coverslips were positioned facing each other, but separated by 2–3 mm using paraffin legs. (*D*) A schematic depicting the transwell set-up. WM983b–GFP cells were cultured in the upper chamber of Transwells of different porosity before being transferred to Transwells containing WM983b cells plated on the bottom chamber. (*E*) smFISH image of β-actin–MBS mRNA present in a mNT formed by a primary β-actin–MBS MEF. (Scale bar: 5 μm.) (*F*) smFISH image of β-actin–MBS mRNA along a mNT formed by an immortalized β-actin–MBS MEF. (Scale bar: 10 μm.) See Dataset S1 for data on the number of cells scored, mean, SEM, and *P* values.

than that observed under coculture conditions using healthy cells, indicating that the release of apoptotic bodies cannot account for mRNA transfer under normal growth conditions. In parallel experiments we used an apoptosis-inducing drug, raptinal (43), to selectively kill donor cells during coculture. Raptinal leads to apoptosis within <2 h by inducing cytochrome *c* release from mitochondria, which in turn activates the apoptotic cascade. Consistent with published results (43), APAF-1–KO (APAF-$1^{-/-}$) MEFs are resistant to short-term (1-h) treatment with the drug, whereas APAF-$1^{+/+}$ cells (e.g., MBS MEFs) were highly sensitive and showed >95% cell death within <2 h. We next cocultured MBS MEFs and APAF-$1^{-/-}$ MEFS for 3 or 12 h and then treated the cells with raptinal for 1 h. Transferred mRNA was detected by smFISH after coculture but before treatment (i.e., at time 0) and at different time points during drug treatment (e.g., 30 min, 1 h) or after drug washout (e.g., 2–6 h). Importantly, the amount of transferred β-actin–MBS mRNA was reduced to very low levels upon raptinal treatment (Fig. S6*A* and Dataset S1). Some MBS MEF cell fragments containing mRNA were detected between cells, suggesting that β-actin–MBS mRNA can be present and remain intact in apoptotic bodies (Fig. S6 *B*, *i*). Likewise, we observed clusters of transferred mRNAs in a few acceptor cells (Fig. S6 *B*, *ii*), suggesting that apoptotic bodies were engulfed by these cells. Nevertheless, the contribution of apoptotic bodies to mRNA transfer appears to be extremely limited and does not contribute to the mechanism observed in healthy cells (Fig. S6*A*). Thus, mRNA transfer in cocultures is not mediated by apoptotic bodies.

mRNA Transfer Occurs via mNT-Like Structures. To test if mRNA transfer requires close proximity or direct contact, cells were plated at a 99:1 ratio of WT to MBS MEFs and cocultured for 24 h. smFISH was performed to determine the amount of β-actin MBS mRNA transferred to either the nearest or distant neighbor cells. Nearest neighbors were defined as those directly proximal to the MBS cells (i.e., residing in the adjacent cell layer), while distal cells constituted those in the surrounding second or third layers. We observed that the number of MBS spots was higher in adjacent cells than in cells located further away (Fig. S7 *A* and *B* and Dataset S1).

Our results indicate that a proximity-based mechanism confers intercellular mRNA transfer. To determine whether mRNAs are transferred directly via known cell–cell contacts (e.g., gap junctions), we treated MBS and WT MEF cocultures with 100 μM carbenoxolone, a gap-junction inhibitor (44), for 60–90 min. However, we found no effect of carbenoxolone upon β-actin–MBS mRNA transfer (Fig. S7*C* and Dataset S1). By eliminating other possibilities (e.g., diffusion or gap junctions), we suspected that mRNA transfer might occur via mNTs. mNTs are long (up to ∼200 μm), thin (0.05–0.5 μm) cellular protrusions that can transfer many types of components from one cell to another (24, 25, 27–35). Indeed, upon examination of our coculture images, we could detect the presence of mRNAs in mNT-like structures (Fig. 4 *E* and *F* and Fig. S8*A*). These images were fairly rare, since the visibility of mNTs (as detected by the background fluorescence of the FISH protocol) was weak. Furthermore, we suspect that many mNTs are destroyed during the FISH process. Indeed, we could detect mNTs more easily by live imaging (see below).

To further substantiate the role of mNTs in mRNA transfer, we employed known mNT inhibitors. It was previously shown that FN-coated glass supports mNT formation better than polylysine (PL)-coated glass (45). Consistent with this finding, we found that cells plated on uncoated or PL-coated glass exhibited much less mRNA transfer than cells plated onto FN-coated glass (Fig. S8*B* and Dataset S1). An alternative explanation for the reduced transfer on PL-coated glass would be that the mRNA-expression levels in the donor cells were greatly reduced. However, the expression levels of β-actin–MBS mRNA in the donor MBS MEFs were only ∼30% less under these conditions (Fig. S1*C*). Next, we tested the effects of the actin depolymerization drug Latrunculin A (LatA) and the CDC42 inhibitor 2-[(2,3,4,9-Tetrahydro-6-phenyl-1*H*-carbazol-1-yl)amino]ethanol (CASIN), which were previously shown to inhibit mNT formation or the transfer of proteins through mNTs (25, 46). Consistent with the involvement of mNTs, we found that treatment of WT or MBS MEF cocultures with either LatA or CASIN resulted in a two-fold reduction in β-actin mRNA transfer (Fig. S8 *C* and *D* and Dataset S1). The reduced level of transfer cannot be attributed

to decreased mRNA levels in donor cells (Fig. S1*C*), and, furthermore, the percentage of transferred mRNA present in LatA-treated cocultures was greatly reduced (Fig. S8*E* and Dataset S1). Thus, mRNA transfer through contact-dependent mNTs seems to be the likely mechanism.

Live Imaging of mRNA Transfer. A great advantage of the MS2-labeling system is the ability to follow mRNA movement in real time by live imaging. Although we could detect transferred β-actin–MBS mRNA in acceptor cells after coculture using both smFISH with probes against MBS and immunofluorescence (IF) using anti-GFP antibodies to detect tandem MCP–GFP (tdMCP–GFP) (47), the number of colabeled spots was very low (Fig. S9*A*). Indeed, the expression of tdMCP–GFP in the donor cells greatly reduced the level of transfer in cocultures (Fig. S9 *B* and *C* and Dataset S1). In contrast, the expression of either tdMCP–GFP in the acceptor cells or of GFP alone in the donor cells did not lower the level of mRNA transfer. Thus, the binding of tdMCP–GFP to β-actin–MBS mRNA in the donor cells appears to inhibit mNT-mediated delivery of mRNA to acceptor cells. While it was difficult to detect transfer by live-cell imaging, we nevertheless documented one clear event of linear β-actin–MBS mRNA transfer between donor and acceptor cells (Fig. 5 *A* and *B* and Movie S1). The rate of β-actin–MBS mRNA movement in Movie S1 was calculated at 4.85 μm/min. This rate is similar to that of other components that transfer via mNTs (48). In addition, we often observed mNTs by live imaging and on rare occasions detected mRNAs moving along the length of mNT-like structures or appearing in acceptor cells using tdMCP–GFP (Fig. 5 *C* and *D* and Fig. S8 *A*, *iii* and Movies S2–S6).

Discussion

Current research suggests that cells secrete RNA molecules into extracellular fluids, which are then taken up by downstream acceptor cells to alter gene expression and, ultimately, cell physiology. Although the evidence for miRNA transfer via EVs or RNP particles is compelling, the evidence for EV-mediated transfer of mRNA is lacking both in qualitative and quantitative terms. Here, we took an unbiased approach to ask whether intact mRNA molecules are transferred between cells. We provide visual evidence and quantitative data showing that mRNA molecules undergo intercellular transfer and that this transfer occurs via mNTs between adjacent cells and not by diffusion (see the model in Fig. 6). This work presents the results of independent studies performed and validated by different research teams.

Do All mRNAs Transfer? The data presented in this study show that essentially all mRNAs tested can undergo transfer between mammalian cells (Figs. 1 and 2 and Fig. S4). This list includes native endogenously expressed mRNAs (e.g., β-actin–MBS, MITF, SERP2, MT2A, BRCA1, and HER2), ectopically expressed mRNAs (e.g., GFP, LTag, CCND1–MBS), as well as MS2 aptamer-tagged mRNAs. These different mRNAs share no known sequence commonalities, nor do their encoded proteins localize and/or function on the same cellular processes or pathways. Moreover, the list includes both nonmammalian (GFP) and viral (LTag) proteins. Overall, the results suggest that perhaps all mRNAs are amenable to transfer. Thus, far, the only exception we have identified is MALAT1, a lncRNA that resides primarily in the nucleus. However, it is unclear whether the lack of MALAT1 transfer is due to its localization or because it is a noncoding RNA. Since use of smFISH has limited our analysis to only a small number of genes, nonbiased genome-wide transfer experiments that necessitate high-throughput approaches, such as RNA-seq or MERFISH (49), are needed to allow the detection of large numbers of individual transcripts. This will allow us to define and quantitate the extent of the RNA transferome via the large-scale identification of transferrable versus non-transferable mRNAs and lncRNAs. Such an approach may help identify *cis* elements or epi-transcriptomic changes that recruit proteins involved in RNA transfer. This may allow us to predict which RBPs associate with transferred mRNAs and thereby facilitate the transfer process. Importantly, our FISH-IF experiment indicates that the tdMCP–GFP protein is not removed from β-actin–MBS mRNA upon transfer (Fig. S9). Thus, cellular proteins involved in transfer might remain bound to the transferred mRNA in acceptor cells, and pulldown of these mRNAs could reveal the identity of these RBPs. Another aspect of

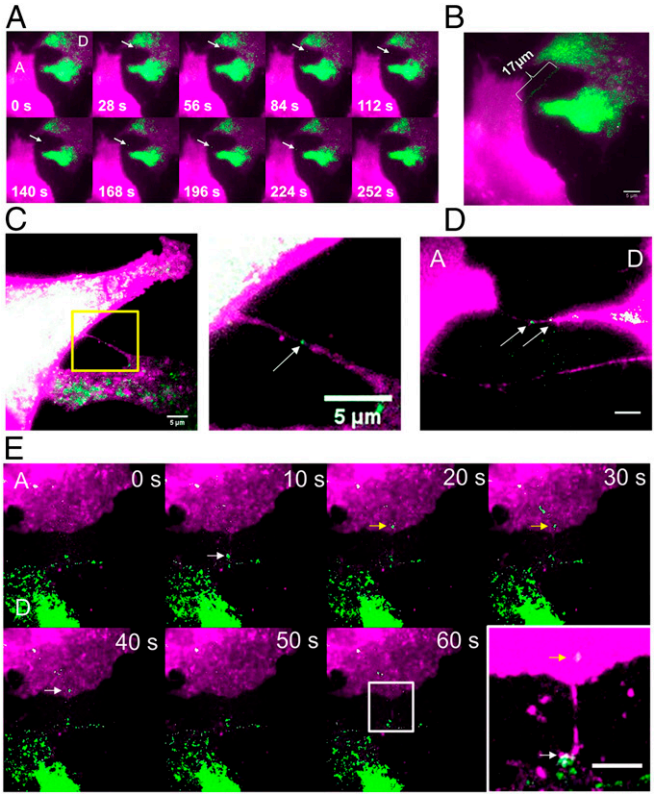

Fig. 5. Live imaging of mRNA transfer. (*A*) Individual time-lapse images from Movie S1 of live imaging of β-actin–MBS mRNA (green) transferring from a donor MBS MEF cell (D) to an acceptor WT MEF cell (A). The membranes of both cells were labeled with TagRFP-T (magenta). The arrow points to a mRNA being transferred. (*B*) Maximum projection of Movie S1. (Scale bar: 5 μm.) (*C*) Live image of a β-actin–mRNA in a nanotube connecting donor MBS MEFs. The image was taken from a coculture of WT acceptor MEFs and donor MBS MEFs expressing tdMCP–GFP showing a mNT that connects two MBS cells. Both cells are labeled with membrane targeted-TagRFP-T (magenta); the arrow points to a tdMCP–GFP–labeled mRNA (green). The image is taken from Movie S2. (Scale bars: 5 μm.) (*D*) Live image of β-actin–MBS mRNAs in a mNT connecting donor and acceptor MEFs. A still image from Movie S4 of cells cultured in *A* shows a mNT that connects a donor MBS MEF (D) with an acceptor WT MEF (A). Both cell types are labeled with membrane-targeted TagRFP-T (magenta); the arrows point to tdMCP–GFP–labeled mRNAs (green). (Scale bars: 5 μm.) (*E*) A time-lapse photomontage that may capture β-actin–MBS mRNA transferring from a donor cell to an acceptor. WT acceptor MEFs (A) and donor MBS MEFs expressing tdMCP–GFP (D) from *A* were cocultured and monitored for mRNA transfer. Images were taken from Movie S5. Arrows point to a tdMCP–GFP–labeled mRNA (green) that appears to transfer between frames (i.e., labeled white in the donor cell and yellow in the acceptor cell). The donor cell is denoted by the green label due to tdMCP–GFP expression but also shows less TagRFP-T label in this case. The image at lower right is a magnified section of a maximum projection of the movie, showing a nanotube-like structure connecting the two cells at the presumed path of the transferring mRNA. Note that in all panels the TagRFP-T (magenta) signal was saturated to enhance the visibility of the nanotube-like structures in the images. (Scale bar: 5 μm.)

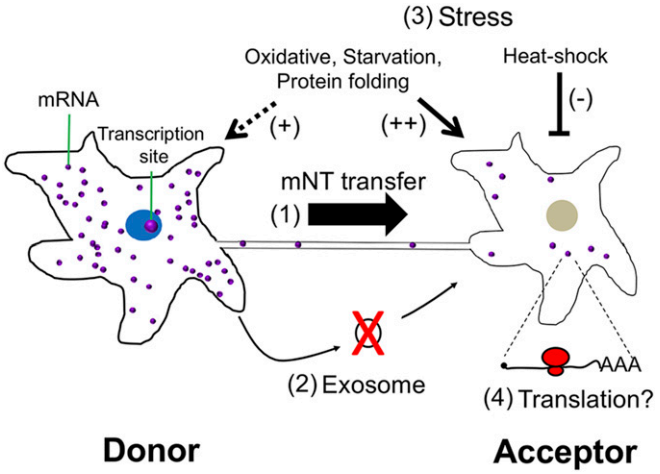

Fig. 6. A schematic representation of intercellular mRNA transfer. (1) A donor cell (*Left*) that expresses a given mRNA can transfer mRNA molecules to an acceptor cell (*Right*) through a mNT. (2) This process appears to be actin-myosin regulated, requires direct physical contact, and does not occur via exosomes. (3) Stress conditions appear to affect mRNA transfer, whereby oxidative, protein-folding, and nutrient stresses on both donor and acceptor cells favor transfer, whereas heat shock of acceptor cells inhibits transfer. (4) Transferred mRNAs are likely to undergo translation, although this has not yet been proven.

selectivity is how, out of the total pool for any given mRNA species, specific mRNA molecules are chosen for transfer. Furthermore, our results suggest that translation does not play a role, since translation inhibition did not affect β-actin–MBS mRNA transfer (Fig. S6).

Is mRNA Transfer Solely Expression Dependent? Two single-cell approaches are used to quantify the number of mRNA transcripts in cells: single-cell RNA sequencing (scRNA-seq) and smFISH. The detection level of scRNA-seq depends upon the methods of single-cell isolation, RNA extraction, and depth of sequencing but may suffer from amplification biases and transcript underestimation compared with spike-in controls (50). Thus, scRNA-seq may not be sensitive enough for accurate detection of <10 mRNA molecules per cell (50). In contrast, mRNA visualization by smFISH allows unbiased measurements at single-molecule resolution while maintaining the integrity of cell structure and conferring spatial resolution of the detected mRNA molecules. By using smFISH as our method of choice, we detected low numbers of transferred mRNA molecules in acceptor cells, the average for many being <10 molecules per cell. In contrast, β-actin–MBS mRNA was exceptional in that hundreds of mRNA molecules per cell could undergo transfer in coculture experiments.

What makes β-actin–MBS mRNA so effective at transfer? One possible explanation is that high levels of β-actin–MBS mRNA expression in donor cells increase the likelihood for transfer. The idea that mRNA transfer correlates with gene expression is further supported by the finding that elevation of CCND1–MBS mRNA, using the CMVp, increased the number of transferred molecules (Fig. 2*F*). However, high gene-expression levels alone may not guarantee higher levels of transfer. For example, we observed similar levels of HER2 mRNA transfer from two different donor lines that had very different levels of expression (Fig. 2*G* and Fig. S2). Likewise, the expression of MITF, MT2A, and SERP mRNAs were differentially expressed in the same donor cells but had an equally low level of transfer (Fig. 2 *C–E* and Fig. S2). We do note, however, that the low levels of transfer in these experiments might have been caused by plating the cells on uncoated glass, which reduces the efficiency of mRNA transfer compared with plating cells on FN-coated glass. This reduces the efficiency of mRNA transfer in comparison with cells plated on FN-coated glass (Fig. S8*B*). That said, the transfer of CCND1–MBS, LTag, BRCA1, and HER2 mRNAs was also relatively low in comparison with β-actin–MBS mRNA, and these cells were plated on FN-coated glass. Therefore, gene expression may be only one factor that determines mRNA transfer.

Aside from gene expression, other factors influence the propensity of a given mRNA to be transferred. These include cell-culture conditions (Fig. S8*B*), acceptor cell stress (Fig. 3), cell-type specificity (e.g., N87 cells vs. SKBR3) (Fig. 2*G* and Fig. S2), sequence elements or epi-transcriptomic modifications, and RBPs specific to the mRNA in question. Other factors may also be considered; for example, promoter elements are known to affect the cytoplasmic fate of mRNAs (51). Hence, it is possible that elements at the CMVp are responsible for the elevated rate of CCND1–MBS mRNA transfer, rather than its elevated expression per se (Fig. 2*F* and Fig. S2). Organellar localization of an mRNA (e.g., nuclear retention) could also affect availability. Furthermore, it is possible that mRNAs involved in mNT formation (e.g., β-actin) or those spatially distributed near mNTs might show a greater propensity for transfer. These issues will have to be resolved in future studies.

MCP–GFP Inhibits mRNA Transfer. The MS2 system has been widely used to image mRNAs within many organisms and cell types (52) and has not been shown to have deleterious effects upon mRNA movement. Furthermore, a mouse model that expresses both β-actin–MBS and MCP–GFP in all cells did not show physiological, developmental, or behavioral defects (53). However, we found that the expression of tdMCP–GFP in donor MBS MEFs inhibited the transfer of β-actin–MBS mRNA (Fig. S9 *B* and *C*). The reduction in RNA transfer cannot be explained by a reduced expression level of β-actin–MBS mRNA, since tdMCP–GFP did not affect steady-state levels (Fig. S1*C*). Time-lapse imaging of hundreds of live cells for varying durations and at various intervals between frames led to only a single clear example of mRNA transfer (Fig. 5 *A* and *B* and Movie S1) and only a few examples of mRNAs residing in mNTs (Fig. 5 *C* and *D* and Fig. S8 *A*, *iii* and Movies S2, S4, and S6). This might explain why transfer was not detected earlier in other studies employing MS2-labeled mRNAs for single-molecule imaging.

While the cause of tdMCP–GFP–mediated inhibition of β-actin–MBS mRNA transfer is not known, we presume that the larger size/mass of the mRNP particle impedes interactions with the transport machinery and/or recruitment into mNTs. Formation of this complex may invariably slow the anterograde movement of mRNA through mNTs in comparison with retrograde transport, leading to a net movement back to the donor cells (Movie S6). Another possibility is that tdMCP–GFP binding to the mRNA results in structural changes in the RNA that interfere with the binding of factors essential for transfer.

Clearly, inhibition of β-actin mRNA transfer between cells is not deleterious at the organismal level, since β-actin–MBS × MCP–GFP crosses are fully viable (53). This is probably because β-actin is ubiquitously expressed in all cell types and therefore is not expected to be limiting. We predict, however, that the inhibition of transfer of other mRNA species might yield more obvious and deleterious effects at both the cellular and organismal levels. The loss of transfer of cell type-specific mRNAs may alter the physiology of downstream acceptor cells, although this will have to be determined on a case-by-case basis.

What Is the Mechanism of mRNA Transfer? Our work demonstrates that mRNA transfer between cells likely occurs via mNT-based contacts and not via diffusion-based mechanisms. However, the mechanisms that regulate mNT formation and maintenance are not well understood. Likewise, even less is known about how mRNAs are recruited to mNTs and undergo trafficking therein.

mNTs are thought to be actin filament-based, but microtubules may also be present and possibly exist as the sole cytoskeletal structure (54). In our study, the inhibition of actin polymerization was found to reduce β-actin–MBS mRNA transfer in cocultured cells (Fig. S8*D*), which implies at least a partial role for actin. The CDC42 small GTPase, which regulates actin filament formation, has also been implicated in mNT formation (25, 55), perhaps in the elongation rather than the initiation phase (56). Nevertheless, the inhibition of CDC42 reduced mRNA transfer (Fig. S8*C*), strengthening our hypothesis that mRNAs transfer via actin-based mNTs.

Other proteins have been shown to modulate mNT formation. For example, TNFaip2/M-Sec utilizes the RalA GTPase and exocyst complex to initiate mNT formation (55, 56) and is recruited along with filamin and myosin to the plasma membrane by the MHC class III protein LST1 (46) to initiate mNT formation. Although it is yet unclear which cytoskeletal motors are responsible for mNT-mediated mRNA transfer, the velocity of the RNP particle shown in Movie S1 strongly resembles that of myosin motors (57, 58). In particular, Myosin Va is involved in RNA trafficking (59) and is probably a good candidate to explore, given that earlier work suggested a role for this motor in the distribution of Schwann cell-synthesized RNA to neuronal cell bodies and axons after lesioning (60). Future experiments employing the knockdown/knockout of specific myosin motors should elucidate which motor confers mNT-mediated mRNA transfer. Although most evidence suggests that mNTs are open-ended and facilitate free cytoplasmic transfer (24–26), an alternative model in which the acceptor cell phagocytoses the tip of the mNT was put forth (30). In that case, the transferred mRNA is expected to initially reside in endosomes after entering the acceptor cells. While we have no clear answer which model is correct, it should be noted that both the open-ended and tip-phagocytosis models require direct cell-to-cell contact by mNTs.

Finally, the question arises of whether mRNAs are transferred in free RNP particles or in particles bound to cellular membranes. Organelles such as intact mitochondria, as well as lysosomes, endosomes, Golgi vesicles, and endoplasmic reticulum (ER), have been shown to transfer via mNTs (24, 31, 61, 62). Likewise, mRNAs are known to associate with and undergo intracellular cotrafficking with organelles (e.g., ER, mitochondria, and peroxisomes) (63–66). Thus, we speculate that organelle-localized mRNAs may undergo transfer along with the organelle. Live imaging of mNT-mediated mRNA transfer using cells expressing labeled organelles should help resolve this issue.

Why Do mRNAs Transfer Between Cells? The biological importance of mRNA transfer between cells is still unknown. Clearly, mRNAs or their fragments are found in EVs and are presumably taken up by the surrounding cell layers in tissues. Our discovery of mNT-mediated mRNA transfer suggests that full-length mRNAs can also be exchanged between cells through contact. Although we cannot rule out the possibility that this phenomenon occurs only under in vitro culture conditions, it would seem unlikely given the existence of mNTs in tissues and their known ability to transfer intracellular material. Thus, we assume that the process of intercellular mRNA transfer is active (i.e., is cytoskeleton- and motor-dependent), is responsive to environmental cues (e.g., stress), and affects downstream cellular responses.

mNTs have been characterized primarily in cell and tissue cultures. However, they were also detected in patient-derived solid tumors (67). This suggests a role for mNTs in cancer biology and the tumor microenvironment. The finding that primary MEFs can be mRNA donors as well as acceptors (Fig. 1 *F* and *G* and Fig. S2*B*) indicates that mRNA transfer is not a consequence of immortalization or tumorigenesis per se. Therefore, this process is expected to occur in embryonic and/or normal adult tissues and may affect development, maintenance, or both. Future studies employing human xenografts in rodents may help resolve this question.

Given that mNT-mediated mRNA transfer occurs in animals, the main biological question is impact the transfer of a few mRNA molecules has upon downstream acceptor cells. The answer depends on the mRNA in question and hinges on whether the transferred mRNA is translated and at what efficiency. For instance, cancer cells that transfer a few mRNA molecules encoding a key transcription factor not normally expressed in untransformed neighbor cells might induce or repress the transcription of genes that regulate responses to extracellular signals elicited from the cancerous cells and thereby facilitate cancer cell motility or the supportive nature of tumor local microenvironment. It is reasonable to speculate that mRNAs with transforming potential (i.e., oncogenes) could induce carcinogenesis in neighboring cells upon transfer. Likewise, the transfer of mRNAs involved in cell differentiation during embryonic development might act as means to induce or repress neighboring cells. Determining the scope of this process and deciphering the mechanism and physiological outcome of mRNA transfer will be the goal of future studies.

Materials and Methods

Cells and Cell Lines. Primary MEFs from WT (C57BL/6) or β-actin–MBS mice were isolated from E14.5 embryos and cultured as is or were immortalized by transfection with SV40 LTag, as previously described (23). Immortalized ZBP1-KO (ZBP1$^{-/-}$)–MBS MEFs were described earlier (38). HEK293T, U2OS, NIH 3T3, and SKBR3 cells were purchased from ATCC. The following cell lines were received as gifts: SKBR3 from M. Oren, Weizmann Institute of Science (hereafter, "WIS"), Rehovot, Israel; U2OS from Z. Livneh, WIS; N87 from Y. Yarden, WIS; WM983b from M. Herlyn, The Wistar Institute, Philadelphia; HEK293 cells expressing P_{CCND1}–CCND1–MBS or P_{CMV}–CCND1–MBS (42) from Y. Shav-Tal, Bar Ilan University, Ramat Gan, Israel; and SV40-immortalized APAF-1–KO MEFs and isogenic WT MEFs (68) from M. Orzáez, Centro de Investigación Príncipe Felipe (CIPF), Valencia, Spain.

MEFs expressing EGFP, NLS–HA–tdMCP–GFP (referred to herein as "tdMCP–GFP") or palmitoylated TagRFP-T (TagRFP-T-ps) were created by infection with the appropriate lentivirus followed by sorting by flow cytometry to isolate only infected cells. Cells were sorted for low expression levels of EGFP and tdMCP–GFP and for high expression levels of TagRFP-T-ps. WM983b–GFP cells were created by clonal selection, as previously described (69).

Plasmids and Lentivirus Generation. A lentivirus vector (pHAGE-UBC-RIG) carrying tdMCP–GFP (Addgene plasmid no. 40649) was previously described (47). DNA sequences encoding EGFP and TagRFP-T-ps were cloned into the same viral backbone vector. Plasma membrane (inner leaflet)-associated TagRFP-T-ps was generated by the addition of a sequence encoding 20 amino acids of rat GAP-43 (MLCCMRRTKQVEKNDEDQKI) (70) to the 5′ end of the TagRFP-T gene.

Lentivirus particles were produced by transfecting the expression vector along with plasmids for ENV (pMD2.VSVG), packaging (pMDLg/pRRE), and REV (pRSV-Rev) (Addgene plasmids nos.12259, 12251, and 12253, respectively) into HEK293T cells using calcium phosphate (71). The virus-containing supernatant was harvested and concentrated using a Lenti-X concentrator (Clontech) per the manufacturer's instructions. Virus particles were resuspended in DMEM containing 10% FBS, aliquoted, and stored at −80 °C for subsequent infection of cells in culture.

Cell-Culture Conditions. MEFs, HEK293, HEK293T, and U2OS cells were cultured routinely in 10-cm dishes in DMEM (4.5 g/L glucose) supplemented with 10% FBS, 1 mM sodium pyruvate, and antibiotics (0.1 mg/mL streptomycin and 10 U/mL penicillin) at 37 °C with 5% CO_2. Primary MEFs were cultured in the same medium at 37 °C with 10% CO_2 and 3% O_2. SKBR3 and N87 cells were cultured in RPMI 1640 medium supplemented with 10% FBS, 1 mM sodium pyruvate, and antibiotics. RPMI 1640 medium was also used for the coculture of either SKBR3 or N87 cells with MEFs that were preconditioned to RPMI 1640. WM983b cells were cultured in Tu 2% medium (78.4% MCDB153 medium, 19.6% Leibovitz's L-15 medium, 2% FBS, and 1.68 mM $CaCl_2$).

FN (10 μg/mL in PBS; Sigma) was used to coat round 18-mm no. 1 glass coverslips for FISH experiments and the glass-bottomed dishes (MatTek catalog no. P35G-1.5–14-C) for live imaging. For some experiments, poly-D-lysine (Sigma) was used to coat coverslips at 1 mg/mL or 0.1 mg/mL, as indicated. Cells were dissociated from the dishes using 0.25% trypsin-EDTA and were plated on freshly coated coverslips. We found that the coculturing of donor and acceptor cells immediately after dissociation tends to

reduce the transfer efficiency of β-actin–MBS mRNA. Therefore, acceptor cells were typically plated the day before coculture (i.e., in the afternoon/evening), and donor cells then were plated on top the next morning, unless otherwise indicated. The acceptor:donor ratio was 1:1 unless otherwise indicated. Coculture was performed for 30 min to 24 h, as indicated, before fixation and FISH analysis as detailed below. For live imaging, cells were cultured on fibronectin-coated glass-bottomed dishes, as described above, using DMEM/10%FBS medium. The coculture was maintained for 1–2 h in the incubator. During that time, the microscope's environmental control chamber was warmed to 37 °C with humidity control and normal atmosphere. The medium was then replaced with prewarmed Leibovitz's L-15 medium lacking phenol red and containing 10% FBS, and the cells were taken for imaging. Imaging sessions of live cells lasted between 1 and 10 h. Experiments using WM983b cells were performed using uncoated glass, and cocultures (plated at a ratio of 1:1) were incubated for 48 h before FISH analysis. In all cases, cell density upon plating in coculture was calculated to achieve ∼80 ± 10% confluence at the time of fixation or live imaging.

For tripod experiments, paraffin was heated to ∼110 °C. By using a glass pipette, paraffin drops (2–3 mm in height) were placed in a triangular arrangement at three points on the coverslip edges. Once the paraffin solidified, coverslips were exposed to UV light (using the tissue-culture hood lamp) for 30 min. Tripods were stored under sterile conditions at room temperature until used. For transwell experiments, Corning Transwell multiple-well plates with permeable polycarbonate 0.4-μm or 5-μm membrane inserts (Fisher Scientific catalog no. 07–200-147 or 07-200-149) were used.

The following drugs were added directly to the culture medium: 100 μg/mL cycloheximide (CHX) (Sigma), 1 μM CASIN (a gift of V. Krizhanovsky, WIS), 200 nM LatA (Santa Cruz Biotechnology), 100 μM carbenoxolone (Sigma), and 10 μM raptinal (gift of P. Hergenrother, University of Illinois Urbana–Champaign, Urbana–Champaign, IL). Drugs were added 20–30 min after plating of the donor cells (i.e., after MBS MEFs have attached). For the induction of protein folding or oxidative stress, 0.1 mM DTT (Sigma) or 1 mM H_2O_2 was added directly to the medium, and cells were further incubated for 1.5 h. Serum starvation was induced by replacing the medium with DMEM lacking FBS, and the cells were further incubated for the indicated times. Heat shock was induced by submerging cells that were precultured on coverslips in a sealed 12-well plate for 1 h in a 42-°C water bath. Following incubation under stress conditions, the stressed cells were washed with prewarmed medium; then the other (nonstressed) cell type was added, and the cells were cocultured for the indicated times under stress-free conditions. For the apoptosis-tripod experiment, cells grown on tripod coverslips were first treated with 3 mM H_2O_2 for 1.5 h before coculture. After an additional 2.5 h of culture in medium lacking H_2O_2, ∼45% of MBS MEFs were dead. The percentage of cell death was determined using trypan blue staining.

FISH and FISH-IF. Tiled FISH probes (20-mers) against the MBS sequence (comprising three oligos with amino-allyl moieties on both the 5′ and 3′ ends) and the β-actin ORF (comprising 35 5′ and 3′ amino-allyl oligos) (23) were end-labeled with Cy3 or Cy5 (GE Healthcare), as previously described (72). Tiled FISH probes (20-mers) against human BRCA1-Quasar (Q)570 (ShipReady catalog no. SMF-2028-1), human HER2-Q570 (DesignReady catalog no. VSMF-2102-5), and custom probe sets against HSP70 (73) and LTag-Q670 mRNAs were obtained from Biosearch Technologies. Tiled odds/evens dual-color 20-mer probes against GFP and human MITF, SERP2, MT2A, and MALAT1 were purchased as 3′-amine oligos from Biosearch Technologies. These oligos were coupled to Cy3 or Alexa Fluor 594 (Life Technologies) fluorophores and purified by HPLC, as previously described (41).

FISH was performed at the R.H.S./J.E.G. laboratories as previously described (22), with slight modifications (a detailed protocol is given in *SI Materials and Methods*). FISH at the A.R. laboratory was performed on WM983b cells according to the Biosearch Stellaris RNA FISH protocol.

For FISH-IF experiments, cell fixation and permeabilization were performed as described for FISH. Prehybridization was performed in prehybridization buffer (PHB) (10% formamide in 2× SSC) supplemented with 3% BSA (Sigma) and RNase inhibitor [10 U/mL SUPERase (Ambion) or RNasin (Promega)]. For hybridization, 20 U/mL SUPERase or RNasin and primary chicken (IgY) anti-GFP antibody (GFP-1010) (1:5,000) (Aves Labs), as well as the FISH probes, were added to the hybridization mix. Samples were incubated in a humid chamber in the dark at 37 °C for exactly 3 h. Following hybridization, coverslips were rinsed twice in PHB and then incubated twice for 30 min at 37 °C in PHB supplemented with 3% BSA and secondary goat anti-chicken IgY antibody conjugated with Alexa Fluor 647 (A21449) (1:1,000) (Life Technologies). Samples were further washed, DAPI stained, and mounted on slides as for FISH.

Imaging. FISH and FISH-IF images were taken using different microscopes, as detailed in *SI Materials and Methods*. Exposure times for imaging varied among different cell cultures, probes, dyes, and microscopes and were determined empirically per experiment. All slides from the same experiment were imaged using the same illumination parameters. Examples of *z*-stacked FISH images of donor, acceptor, and cocultured cells are provided in Movies S7–S9). Live imaging was performed on an Olympus IX-71 total internal reflection fluorescence (TIRF) station customized for laser illumination as detailed in *SI Materials and Methods*.

Image Analysis and Data Presentation. Microscope images presented in the figures and movies were minimally processed for brightness and contrast using the FIJI program (74). The plots depicted in Fig. S3*E* were generated in FIJI by using the "straight line" tool to measure pixel intensity. Analysis of smFISH images to quantify FISH spots was performed using either in-house–developed MATLAB programs or FQ (36). Airlocalize (23) was used at the R.H.S. laboratory for the experiments depicted in Figs. 1 *D* and *E* and 4*A* and Fig. S7*B*. All experiments involving WM983b cells were analyzed at the A.R. laboratory with Rajlabimagetools (75). FQ was used in the analysis of all other experiments. For more details, see *SI Materials and Methods*. Examples of images that were analyzed by FQ are provided in Figs. S1 *A* and *B* and S10. The data presented in all graphs and in Dataset S1 represent data collected from two or more experiments. In a few cases that showed distinct subpopulations (i.e., Figs. S3 *A* and *B* and S6*A*) the different experiments were color-coded. The immortalized data in Fig. S1*C* were pooled from all experiments with MBS MEFs.

Statistical Analysis. Unpaired *t* tests were used to calculate *P* values (depicted in Dataset S1) for each two sets of compared results. All calculations of average, SEM, and *P* values were performed using GraphPad Prism software (GraphPad Software, Inc.).

ACKNOWLEDGMENTS. We thank Xiuhua Meng and Bin Wu for plasmids; Yaron Shav-Tal, Moshe Oren, Yosef Yarden, Meenhard Herlyn, and Maria Orzáez for cell lines; Paul Hergenrother for raptinal; Valery Krizhanovsky for CASIN; Shalev Itzkovitz for use of his microscopes; and Florian Mueller for excellent technical support for FISH-quant. G.H. is a recipient of a Gruss Lipper Family Post-Doctoral Fellowship from the EGL Charitable Foundation, Dean of Faculty (Weizmann Institute of Science) and Sir Charles Clore Post-Doctoral Fellowships, and Koshland Foundation and McDonald-Leapman Grant Senior Post-Doctoral Fellowships. This research was funded by grants from the Joel and Mady Dukler Fund for Cancer Research (Weizmann Institute of Science) (to J.E.G.); US-Israel Binational Science Foundation-National Science Foundation Grant 2015846 (to J.E.G. and R.H.S.); NIH New Innovator Grant 1DP2OD008514 (to A.R.); and NIH Grant NS083085 (to R.H.S.).

1. Kolodny GM (1971) Evidence for transfer of macromolecular RNA between mammalian cells in culture. *Exp Cell Res* 65:313–324.
2. Kolodny GM (1972) Cell to cell transfer of RNA into transformed cells. *J Cell Physiol* 79: 147–150.
3. Kolodny GM, Culp LA, Rosenthal LJ (1972) Secretion of RNA by normal and transformed cells. *Exp Cell Res* 73:65–72.
4. Valadi H, et al. (2007) Exosome-mediated transfer of mRNAs and microRNAs is a novel mechanism of genetic exchange between cells. *Nat Cell Biol* 9:654–659.
5. Arroyo JD, et al. (2011) Argonaute2 complexes carry a population of circulating microRNAs independent of vesicles in human plasma. *Proc Natl Acad Sci USA* 108: 5003–5008.
6. Eldh M, et al. (2010) Exosomes communicate protective messages during oxidative stress; possible role of exosomal shuttle RNA. *PLoS One* 5:e15353.
7. Xiao D, et al. (2012) Identifying mRNA, microRNA and protein profiles of melanoma exosomes. *PLoS One* 7:e46874.
8. Eirin A, et al. (2014) MicroRNA and mRNA cargo of extracellular vesicles from porcine adipose tissue-derived mesenchymal stem cells. *Gene* 551:55–64.
9. Jiang H, Li Z, Li X, Xia J (2015) Intercellular transfer of messenger RNAs in multiorgan tumorigenesis by tumor cell-derived exosomes. *Mol Med Rep* 11:4657–4663.
10. Lee C, et al. (2012) Exosomes mediate the cytoprotective action of mesenchymal stromal cells on hypoxia-induced pulmonary hypertension. *Circulation* 126:2601–2611.
11. Lopez-Verrilli MA, Picou F, Court FA (2013) Schwann cell-derived exosomes enhance axonal regeneration in the peripheral nervous system. *Glia* 61:1795–1806.
12. Tomasoni S, et al. (2013) Transfer of growth factor receptor mRNA via exosomes unravels the regenerative effect of mesenchymal stem cells. *Stem Cells Dev* 22: 772–780.
13. Kanada M, et al. (2015) Differential fates of biomolecules delivered to target cells via extracellular vesicles. *Proc Natl Acad Sci USA* 112:E1433–E1442.
14. Tian T, et al. (2013) Dynamics of exosome internalization and trafficking. *J Cell Physiol* 228:1487–1495.

15. Heusermann W, et al. (2016) Exosomes surf on filopodia to enter cells at endocytic hot spots, traffic within endosomes, and are targeted to the ER. *J Cell Biol* 213:173–184.
16. Batagov AO, Kurochkin IV (2013) Exosomes secreted by human cells transport largely mRNA fragments that are enriched in the 3′-untranslated regions. *Biol Direct* 8:12.
17. Hung ME, Leonard JN (2016) A platform for actively loading cargo RNA to elucidate limiting steps in EV-mediated delivery. *J Extracell Vesicles* 5:31027.
18. Shurtleff MJ, et al. (2017) A broad role for YBX1 in defining the small non-coding RNA composition of exosomes. *bioRxiv*, 10.1101/160556.
19. Chevillet JR, et al. (2014) Quantitative and stoichiometric analysis of the microRNA content of exosomes. *Proc Natl Acad Sci USA* 111:14888–14893.
20. Stevanato L, Thanabalasundaram L, Vysokov N, Sinden JD (2016) Investigation of content, stoichiometry and transfer of miRNA from human neural stem cell line derived exosomes. *PLoS One* 11:e0146353.
21. Raj A, van den Bogaard P, Rifkin SA, van Oudenaarden A, Tyagi S (2008) Imaging individual mRNA molecules using multiple singly labeled probes. *Nat Methods* 5: 877–879.
22. Femino AM, Fay FS, Fogarty K, Singer RH (1998) Visualization of single RNA transcripts in situ. *Science* 280:585–590.
23. Lionnet T, et al. (2011) A transgenic mouse for in vivo detection of endogenous labeled mRNA. *Nat Methods* 8:165–170.
24. Rustom A, Saffrich R, Markovic I, Walther P, Gerdes HH (2004) Nanotubular highways for intercellular organelle transport. *Science* 303:1007–1010.
25. Biran A, et al. (2015) Senescent cells communicate via intercellular protein transfer. *Genes Dev* 29:791–802.
26. Wang ZG, et al. (2012) Myosin-driven intercellular transportation of wheat germ agglutinin mediated by membrane nanotubes between human lung cancer cells. *ACS Nano* 6:10033–10041.
27. Abounit S, Zurzolo C (2012) Wiring through tunneling nanotubes–From electrical signals to organelle transfer. *J Cell Sci* 125:1089–1098.
28. Roberts KL, Manicassamy B, Lamb RA (2015) Influenza A virus uses intercellular connections to spread to neighboring cells. *J Virol* 89:1537–1549.
29. Thayanithy V, Dickson EL, Steer C, Subramanian S, Lou E (2014) Tumor-stromal cross talk: Direct cell-to-cell transfer of oncogenic microRNAs via tunneling nanotubes. *Transl Res* 164:359–365.
30. Wang X, Gerdes HH (2012) Long-distance electrical coupling via tunneling nanotubes. *Biochim Biophys Acta* 1818:2082–2086.
31. Wang X, Gerdes HH (2015) Transfer of mitochondria via tunneling nanotubes rescues apoptotic PC12 cells. *Cell Death Differ* 22:1181–1191.
32. Wang X, Veruki ML, Bukoreshtliev NV, Hartveit E, Gerdes HH (2010) Animal cells connected by nanotubes can be electrically coupled through interposed gap-junction channels. *Proc Natl Acad Sci USA* 107:17194–17199.
33. Wang X, et al. (2016) Rescue of brain function using tunneling nanotubes between neural stem cells and brain microvascular endothelial cells. *Mol Neurobiol* 53: 2480–2488.
34. Wang Y, Cui J, Sun X, Zhang Y (2011) Tunneling-nanotube development in astrocytes depends on p53 activation. *Cell Death Differ* 18:732–742.
35. Zhu S, Victoria GS, Marzo L, Ghosh R, Zurzolo C (2015) Prion aggregates transfer through tunneling nanotubes in endocytic vesicles. *Prion* 9:125–135.
36. Mueller F, et al. (2013) FISH-quant: Automatic counting of transcripts in 3D FISH images. *Nat Methods* 10:277–278.
37. Hüttelmaier S, et al. (2005) Spatial regulation of beta-actin translation by Src-dependent phosphorylation of ZBP1. *Nature* 438:512–515.
38. Katz ZB, et al. (2012) β-Actin mRNA compartmentalization enhances focal adhesion stability and directs cell migration. *Genes Dev* 26:1885–1890.
39. Buxbaum AR, Wu B, Singer RH (2014) Single β-actin mRNA detection in neurons reveals a mechanism for regulating its translatability. *Science* 343:419–422.
40. Yoon YJ, et al. (2016) Glutamate-induced RNA localization and translation in neurons. *Proc Natl Acad Sci USA* 113:E6877–E6886.
41. Cabili MN, et al. (2015) Localization and abundance analysis of human lncRNAs at single-cell and single-molecule resolution. *Genome Biol* 16:20.
42. Yunger S, Rosenfeld L, Garini Y, Shav-Tal Y (2010) Single-allele analysis of transcription kinetics in living mammalian cells. *Nat Methods* 7:631–633.
43. Palchaudhuri R, et al. (2015) A small molecule that induces intrinsic pathway apoptosis with unparalleled speed. *Cell Rep* 13:2027–2036.
44. Tang EH, Vanhoutte PM (2008) Gap junction inhibitors reduce endothelium-dependent contractions in the aorta of spontaneously hypertensive rats. *J Pharmacol Exp Ther* 327: 148–153.
45. Sowinski S, Alakoskela JM, Jolly C, Davis DM (2011) Optimized methods for imaging membrane nanotubes between T cells and trafficking of HIV-1. *Methods* 53:27–33.
46. Schiller C, et al. (2013) LST1 promotes the assembly of a molecular machinery responsible for tunneling nanotube formation. *J Cell Sci* 126:767–777.
47. Wu B, Chao JA, Singer RH (2012) Fluorescence fluctuation spectroscopy enables quantitative imaging of single mRNAs in living cells. *Biophys J* 102:2936–2944.
48. Davis DM, Sowinski S (2008) Membrane nanotubes: Dynamic long-distance connections between animal cells. *Nat Rev Mol Cell Biol* 9:431–436.
49. Moffitt JR, et al. (2016) High-throughput single-cell gene-expression profiling with multiplexed error-robust fluorescence in situ hybridization. *Proc Natl Acad Sci USA* 113:11046–11051.
50. Svensson V, et al. (2017) Power analysis of single-cell RNA-sequencing experiments. *Nat Methods* 14:381–387.
51. Haimovich G, Choder M, Singer RH, Trcek T (2013) The fate of the messenger is predetermined: A new model for regulation of gene expression. *Biochim Biophys Acta* 1829:643–653.
52. Buxbaum AR, Haimovich G, Singer RH (2015) In the right place at the right time: Visualizing and understanding mRNA localization. *Nat Rev Mol Cell Biol* 16:95–109.
53. Park HY, et al. (2014) Visualization of dynamics of single endogenous mRNA labeled in live mouse. *Science* 343:422–424.
54. Austefjord MW, Gerdes HH, Wang X (2014) Tunneling nanotubes: Diversity in morphology and structure. *Commun Integr Biol* 7:e27934.
55. Hase K, et al. (2009) M-Sec promotes membrane nanotube formation by interacting with Ral and the exocyst complex. *Nat Cell Biol* 11:1427–1432.
56. Ohno H, Hase K, Kimura S (2010) M-Sec: Emerging secrets of tunneling nanotube formation. *Commun Integr Biol* 3:231–233.
57. Ropars V, et al. (2016) The myosin X motor is optimized for movement on actin bundles. *Nat Commun* 7:12456.
58. Milo R, Phillips R (2016) *Cell Biology by the Numbers* (Garland Science, Taylor & Francis Group LLC, New York).
59. McCaffrey MW, Lindsay AJ (2012) Roles for myosin Va in RNA transport and turnover. *Biochem Soc Trans* 40:1416–1420.
60. Sotelo JR, et al. (2013) Myosin-Va-dependent cell-to-cell transfer of RNA from Schwann cells to axons. *PLoS One* 8:e61905.
61. Pasquier J, et al. (2013) Preferential transfer of mitochondria from endothelial to cancer cells through tunneling nanotubes modulates chemoresistance. *J Transl Med* 11:94.
62. Rogers RS, Bhattacharya J (2013) When cells become organelle donors. *Physiology (Bethesda)* 28:414–422.
63. Haimovich G, Cohen-Zontag O, Gerst JE (2016) A role for mRNA trafficking and localized translation in peroxisome biogenesis and function? *Biochim Biophys Acta* 1863:911–921.
64. Kraut-Cohen J, Gerst JE (2010) Addressing mRNAs to the ER: Cis sequences act up! *Trends Biochem Sci* 35:459–469.
65. Lesnik C, Golani-Armon A, Arava Y (2015) Localized translation near the mitochondrial outer membrane: An update. *RNA Biol* 12:801–809.
66. Weis BL, Schleiff E, Zerges W (2013) Protein targeting to subcellular organelles via MRNA localization. *Biochim Biophys Acta* 1833:260–273.
67. Lou E, et al. (2012) Tunneling nanotubes provide a unique conduit for intercellular transfer of cellular contents in human malignant pleural mesothelioma. *PLoS One* 7: e33093.
68. Sancho M, et al. (2014) Altered mitochondria morphology and cell metabolism in Apaf1-deficient cells. *PLoS One* 9:e84666.
69. Padovan-Merhar O, et al. (2015) Single mammalian cells compensate for differences in cellular volume and DNA copy number through independent global transcriptional mechanisms. *Mol Cell* 58:339–352.
70. Sanders TA, Llagostera E, Barna M (2013) Specialized filopodia direct long-range transport of SHH during vertebrate tissue patterning. *Nature* 497:628–632.
71. Follenzi A, Naldini L (2002) Generation of HIV-1 derived lentiviral vectors. *Methods Enzymol* 346:454–465.
72. Zenklusen D, Singer RH (2010) Analyzing mRNA expression using single mRNA resolution fluorescent in situ hybridization. *Methods Enzymol* 470:641–659.
73. Vera M, et al. (2014) The translation elongation factor eEF1A1 couples transcription to translation during heat shock response. *Elife* 3:e03164.
74. Schindelin J, et al. (2012) Fiji: An open-source platform for biological-image analysis. *Nat Methods* 9:676–682.
75. Rajlabimagetools. Available at https://bitbucket.org/arjunrajlaboratory/rajlabimagetools/wiki/Home. Accessed October 1, 2015.